Free-Solution, Label-Free Protein-Protein Interactions Characterized by Dynamic Light Scattering

Amy D. Hanlon,* Michael I. Larkin,* and Ryan M. Reddick
Department of Research and Development, Wyatt Technology, Santa Barbara, California

ABSTRACT We report a free-solution, label-free method for quantitative characterization of macromolecular interactions using dynamic light scattering, a temperature controlled plate reader, and a multiwell concentration gradient. This nondestructive technique enabled determination of stoichiometry of binding, equilibrium dissociation constant, and thermodynamic parameters, as well as the impact of temperature, buffer salinity, and a small-molecule inhibitor. The low volume capability of dynamic light scattering reduced the required sample to 426 pmol/experiment, with detection limits for 150-kDa proteins anticipated to be in the low femtomole range.

INTRODUCTION

DNA replication, transcription, mRNA translation, protein degradation, signal transduction, etc., are all enacted by networks of interacting protein complexes. These multicomponent complexes are often transient and reversible, assembling and disassembling rapidly, rearranging and reassembling for the next required activity. Such interactions are intensively studied, not only to gain understanding of cellular function, but also for pharmaceutical development. In vitro, such complexes may be difficult to separate and analyze in pure form, as they equilibrate rapidly with their component monomers and partially formed complexes. Accordingly, methods that evaluate reversible interactions at true equilibrium are indispensable. Since any modification of the protein, either by immobilization or by labeling, can influence the interaction, free-solution, label-free methods are optimal. However, methods meeting these criteria—sedimentation equilibrium analytical ultracentrifugation, isothermal titration calorimetry, and, more recently, concentration-gradient static light scattering (1–4)—all require a relatively large quantity of sample when used in their standard configurations, and are not ideally suited for high-throughput measurement.

In contrast, we now demonstrate a dynamic light scattering (DLS) (5,6) method, concentration-gradient DLS, which enables accurate and quantitative characterization of protein-protein interactions in a high-throughput manner, using only picomoles of sample. DLS, also known as quasi-elastic light scattering or photon correlation spectroscopy, processes the time-dependent fluctuations in scattered light to yield the hydrodynamic radius, r_h, of particles in solution. The hydrodynamic radius is the radius of a solid sphere with the same translational diffusion coefficient as that measured for the sample particle. Relative to static light scattering, which is based upon the absolute intensity of scattered light, DLS is insensitive to background light from the walls of the containing structures. This insensitivity recently permitted DLS measurements from microtiter plates, enabling thousands of sample measurements to be programmed for a single run. The high-throughput capability is a significant improvement over standard DLS single-sample cuvette-based measurements. Over the past four decades, standard DLS has been used in a small handful of independent studies to determine equilibrium dissociation constants of biomolecules (7–11). Although similar in spirit to the work described here, these studies were quite different in detail. Unique to our method is the ability to detect and characterize binding stoichiometries beyond simple dimerization, the demonstrated small-molecule inhibition of protein-protein interactions, and the high-throughput capability. We also demonstrate how both static and dynamic light scattering data can be simultaneously collected and fit to further increase the precision of DLS results. Moreover, we have reduced protein requirements by several orders of magnitude. Together, these developments make DLS characterization of protein-protein interactions practical.

MATERIALS AND METHODS

Materials

We chose to work with proteins that were inexpensive and commercially available. α-chymotrypsin (25.5 kDa) and soybean trypsin inhibitor (Kunitz type, rather than Bowman-Birk type) (21.5 kDa) were obtained from Worthington Biochemical (Lakewood, NJ). Trypsin inhibitor from bovine pancreas, type I-P, essentially salt-free (6.5 kDa), lysozyme (14.7 kDa), and 4-(2-aminoethyl) benzene-sulfonyl fluoride hydrochloride (AEBSF) were obtained from Sigma Aldrich (St. Louis, MO). Phosphate-buffered saline (PBS) solution (10×) was obtained from Fisher Scientific (Hampton, NH). All water was obtained from a Barnstead NANOpure ultrapure water system (Barnstead/Thermolyne, Dubuque, IA), dispensed at 18.3 MΩ-cm. Buffers, microtiter plates, and sample volumes differed with experiment. Experiments involving soybean trypsin inhibitor used 50 mM phosphate, 200 mM NaCl PBS, pH 6.70, a Corning 3540 plate (Corning, NY) for the 10-μL sample volumes and a Corning 3850 plate for the 1-μL sample volumes. Experiments involving bovine pancreatic trypsin inhibitor used 1× PBS (Fisher Scientific), with addition of 250 mM NaCl, pH 7.3,

Submitted May 5, 2009, and accepted for publication September 28, 2009.

*Correspondence: ahanlon@wyatt.com or mlarkin@wyatt.com

Editor: Doug Barrick.

0006-3495/10/01/0297/8 $2.00

doi: 10.1016/j.bpj.2009.09.061

a Corning 3540 plate, and 30-μL sample volumes. Experiments involving chymotrypsin self-association used a 10-mM acetate buffer with varying salinity (50–500 mM NaCl), pH 4.10, a Corning 3540 plate, and 30-μL sample volumes. The lysozyme-chymotrypsin control used 1× Fisher Scientific PBS, with addition of 250 mM NaCl, pH 7.3, a Greiner Bio-one 783892 plate (Greiner, Monroe, NC), and 30-μL sample volumes. The flowing experiment involving simultaneous collection of both dynamic and static light scattering data used Fisher PBS modified with an additional 250 mM NaCl, and 2-mL injections.

Experimental procedures

All sample solutions with the exception of the salt-free bovine pancreatic trypsin inhibitor were desalted/dialyzed using 5 mL HiTrap desalting columns (GE Healthcare Life Sciences) according to manufacturer's specifications. Samples requiring dialysis were made at 3× concentration, desalted, and diluted to the desired concentration. All solutions were filtered through three in-line 0.02-μm Anotop syringe-tip filters, with the exception of the flowing experiment, for which samples were filtered through only one filter. Sample concentration was measured with an Optilab rEX differential refractive-index detector (Wyatt Technology, Santa Barbara, CA) at 660 nm using a *dn/dc* of 0.185 mL/g, or an Ultrospec 4000 UV/Vis spectrophotometer (Pharmacia Biotech, Sunnyvale, CA). Absorption coefficients $A^{1\%}_{280nm}$ of 25.5, 20.4, and 9.94 were used for lysozyme, chymotrypsin, and soybean trypsin inhibitor, respectively. With the exception of the self-association study, we performed our DLS experiments with 500 μg mL^{-1} stock solutions. Lower concentrations may be used, particularly for larger proteins that scatter more light, such as antibodies (r_h =~5–7 nm), which may have stock solutions of 10–20 μg mL^{-1}. All solutions were stored at 4°C for a maximum of 5 h before use.

The buffer viscosity was taken as $\eta_{buffer} = \eta_{water}(1 + \eta_{sp})$, where η_{water} is the viscosity of pure water and η_{sp} is the specific viscosity. The viscosity of water with temperature was taken as $\eta_{water} = 1.66807 \times 10^{12}/T^4 - 1.93927 \times 10^{10}/T^3 + 8.51560 \times 10^7/T^2 - 1.66696 \times 10^5/T + 1.22641 \times 10^2$, where η is in cP and T is in Kelvin. Buffer η_{sp} values were measured for all experiments, with the exception of the buffer used for the bovine pancreatic trypsin inhibitor and lysozyme experiments. In these cases, the specific viscosity was calculated, using Sednterp (University of New Hampshire, Durham, NH) software (reference date 10/7/1994), to be 0.03932, and it was assumed that this viscosity did not vary with temperature. Buffer η_{sp} values were measured against degassed nanopure water with a Wyatt Technology ViscoStar viscometer, using an LC 20AB Prominence HPLC pump (Shimadzu, Kyoto, Japan) or Agilent 1100 series HPLC pump (Agilent, Santa Clara, CA) to maintain a flow of 0.5–1 mL min^{-1} of NANOpure water, and a Wyatt Technology *dn/dc* injector kit equipped with either a 1- or 2-mL sample loop. Wyatt Technology ASTRA software was used to collect and analyze data. Three injections were made for each buffer at each temperature, as shown in Fig. S1 *a* in the Supporting Material. The average measured specific viscosity value was used for calculations. The pH 4.10 self-association buffer specific viscosity was found to vary with NaCl concentration as $0.00229 + 0.08498 \times$ ([NaCl] (M)), with $R^2 = 0.99995$, where R^2 is the coefficient of determination (Fig. S1 *b*). The α-chymotrypsin-soybean trypsin inhibitor buffer specific viscosity was found to have a slight temperature dependence, as $-4.72 \times 10^{-6} \times T^2 + 3.08\text{x}10^{-3} \times T - 4.56 \times 10^{-1}$, with $R^2 = 0.99965$, where T is in Kelvin (data not shown).

For all experiments, two stock solutions were used to compose up to 20 solutions, ranging from 0% *A*:100% *B* to 100% *A*:0% *B*. For self-association studies, *A* represented stock solution and *B* buffer.

For collection of DLS data, concentration-gradient solution series were pipetted into a microtiter plate in randomized quintuplicate (Fig. 1). Plates were covered and subjected to a 15-s 1000 × *g* centrifugation in a TJ centrifuge (Beckman Instruments, Fullerton, CA). This centrifugation removed trapped air/bubbles from the sample. Paraffin oil (1–15 μL) was then deposited on each well, and the plate was recentrifuged at 1000 × *g* for 15 s and placed in a Wyatt Technology DynaPro temperature-controlled plate reader. Wyatt Technology Dynamics software was used to schedule the measurements and collect the data. Each well was measured 50 times, with 1-s acquisitions. This resulted in 250 measurements for each member of the concentration-gradient solution series.

For simultaneous collection of both dynamic and static light scattering data, the two stock solutions were mixed and injected by a Wyatt Technology Calypso automated syringe pump system, which was programmed to inject the entire concentration gradient. Injections of 2 mL were used for each step in the gradient, with both protein stock solutions having concentrations of ~250 μg mL^{-1}. This corresponded to ~10 mg of protein. A temperature-controlled Wyatt Technology DAWN HELEOS II equipped with Wyatt Technology internal WyattQELS was used to measure both static and dynamic light scattering at 25°C. A Wyatt Technology Optilab rEX differential refractometer was used to monitor concentration. Data were collected using Wyatt Technology ASTRA software and exported for analysis in a custom program written in C++.

Data processing

After fitting the autocorrelation functions from each sample, a postfitting data filter was applied (Fig. S2). The filter settings were an autocorrelation function fitting range of 2 μs to 0.08 s (118 points of measurement), a maximum sum of squares deviation of 1 between autocorrelation function

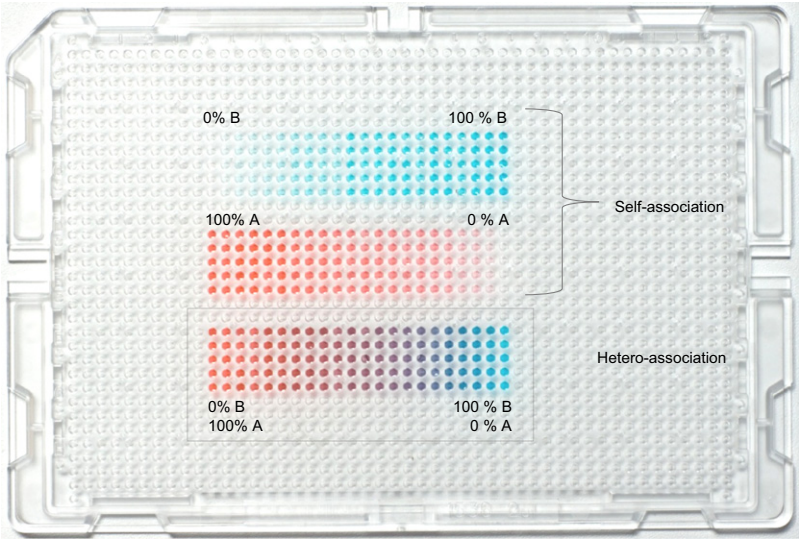

FIGURE 1 Photograph showing examples of concentration gradients in a 1536-well plate with 2 μL sample volume. Three experiments, repeated in quintuplicate, were artificially colored and shown with nonrandomized placement for the sake of demonstration. Protein *A* is red; protein *B* is blue. Self-association experiments are shown above the heteroassociation experiment.

data and fit, a minimum autocorrelation function amplitude of 0.03, a maximum autocorrelation function amplitude of 2, a maximum autocorrelation function baseline of 1.005. When the acquisitions did not meet the filter criteria, they were culled and the data refit. Data sets were subsequently exported to the software program Microsoft Excel, where a custom macro was used to organize and cull the data. Measurements with hydrodynamic radius values >1–2 standard deviations from the average value were culled. Measurements with autocorrelation function amplitude values of outside 2 standard deviations were also culled. The culling, in combination with the Dynamics software data filter, removed measurements contaminated with dust, bubbles, or plate imperfections. Bovine pancreatic trypsin inhibitor data sets were also culled to produce an even data distribution as a function of mole fraction. "Mole fraction" refers to the ratio of molar concentrations, $[A]/([A] + [B])$.

All experiments involving measurements at multiple temperatures were subjected to a postexperimental temperature calibration. Calibration was based on normalization of measured hydrodynamic radii at mole fraction endpoint values of 0 and/or 1, representing 100% protein *B* and 100% protein *A*, respectively. Previous work (data not shown) had shown that self-association did not occur in either buffer for any of the three proteins under the conditions of the multiple-temperature experiments. Normalization accounted for any minor inaccuracies in the measured versus actual temperature, which would result in inaccurate r_h values (Eq. 3). The values of hydrodynamic radii for both the α-chymotrypsin/lysozyme experiment and the simultaneous DLS/static light scattering experiment were also adjusted based on endpoint normalization to known values. As discussed in the Experimental method section, culled data were then fit with different stoichiometry models using a custom C++ program to extract K_d, α parameter (discussed below), and thermodynamic parameters. Different stoichiometry models were compared by visual appearance and reduced χ^2 value, where reduced χ^2 is the sum of squares of the deviation between the fit and the data, divided by the number of degrees of freedom in the fit.

Experimental method

For the characterization of the interaction of two different proteins, we used a variation of the experimental method known in the literature as the Method of Continuous Variation, or the Job Plot (12,13). This technique holds the total molar concentration of the two components constant, while varying their mole fraction. A measurable parameter proportional to complex formation, such as ultraviolet-visible absorption or enzymatic activity, is plotted against the mole fraction of the two components. Here, we used the average hydrodynamic radii, r_{avg}, as the measurable parameter.

For a mixture of proteins in solution, if the proteins do not interact, the measured r_{avg} of the mole fraction series does not increase beyond the values expected for a solution of mixed monomers. If proteins *A* and *B* associate, there will be an increase in the measured r_{avg} beyond this level. A simple 1:1 interaction will have a maximum increase in hydrodynamic radius at 0.5 mol fraction, the ratio with an equal proportion of *A* and *B* in solution. A simple 1:2 interaction will exhibit a maximum at <0.5, whereas a simple 2:1 will exhibit a maximum at >0.5, etc (12).

For characterization of self-association, we used a simplified version of the Method of Continuous Variation, and measured r_{avg} as a function of molar concentration. r_{avg} is expected to increase with total concentration for a self-associating system. To the best of our knowledge, this article demonstrates the first application of the Method of Continuous Variation to DLS. In addition to binding stoichiometry, we also used the technique to estimate the complex size(s) and K_d values.

To measure r_{avg}, a cumulants type analysis was used. There are two common methods used when analyzing autocorrelation functions, cumulants and regularization (14,15). Regularization analysis estimates the distribution of species sizes that would yield the measured autocorrelation function. In this sense, regularization would be ideal for determining how much monomer and complex (and thereby yielding the K_d) are present in solution. However, regularization analysis is limited in resolution. Individual species must differ in hydrodynamic radius by a factor of 4–5 before they are found to be distinct species, rather than one species of intermediate radius. Typically, protein-protein interactions do not result in species with such disparate sizes, and the utility of regularization analysis is thus reduced in this context. Cumulants analysis also determines an intermediate hydrodynamic radius based on all species present in solution. In contrast to regularization, however, the contributions from the constituent species to the measured hydrodynamic radius are well defined in cumulants analysis. This makes modeling of the species present in solution straightforward, and cumulants analysis clearly the best choice for protein interaction data. Dynamics software fit the DLS autocorrelation functions to a cumulants-type function (Part 3 in the Supporting Material), truncated at the second cumulant term, with the physically impossible negative correlation rates disallowed. The resulting functional form is given in Eq. S15.

Cumulants analysis determines an average translational diffusion coefficient, D_z, where the subscript z indicates weighting by the relative intensity of light scattered by each species, as

$$D_z = \sum_i I_i D_{T,i}, \tag{1}$$

where $D_{T,i}$ represents the translational diffusion coefficients for each species and I_i the relative scattering intensities from each species (14,16). For species <~20 nm in radius, there is no significant angular dependence to the intensity of scattered light from the samples, and the intensity of light scattered from a single species is proportional to the molar mass squared times the molar concentration (17). Equation 1 therefore becomes

$$D_z = \frac{\sum_i M_i^2 c_i D_{T,i}}{\sum_i M_i^2 c_i}. \tag{2}$$

Hydrodynamic radius is calculated from the translational diffusion coefficient using the Stokes-Einstein relation (Eq. 3)

$$r_h = \frac{k_B T}{6\pi\eta D_T}. \tag{3}$$

Here, k_B is the Boltzmann constant, T is temperature in Kelvin, and η is viscosity (6). Using Eq. 3 to convert the diffusion coefficients to radii, and canceling common terms, we have

$$r_{avg} = \frac{\sum_i M_i^2 c_i}{\sum_i M_i^2 c_i / r_i}, \tag{4}$$

where r_i represents the hydrodynamic radii of the individual species. The r_{avg} given in Eq. 4 is the cumulants "r_h" value reported by most DLS analysis software. In this work, we use the "avg" subscript as a convenient reminder that the reported value results from cumulants analysis of the autocorrelation function, and may represent the average of several species. From Eq. 4, it is clear that the measured average hydrodynamic radius may be modeled using molar masses, molar concentrations, and radii of the constituent species.

Although a single measurement of r_{avg} obviously cannot characterize the mixture of species present in solution, multiple measurements over a series of concentrations can result in an accurate characterization. This is the underlying principle of the Method of Continuous Variation. In this study, for every member of the concentration series, the measured r_{avg} was fit against the r_{avg} modeled for a proposed stoichiometry. Molar masses of the monomers were obtained from the vendors. Molar concentrations of monomer and complex in solution were modeled using standard chemical equilibrium relations and the known total concentrations of *A* and *B*; The K_d and the complex hydrodynamic radii were left as free parameters in the fit. For example, for the postulated reaction $A + B \rightleftarrows AB$, the total amount of protein in solution is a mixture of monomer and complex: $[A_{tot}] = [A] + [AB]$, and $[B_{tot}] = [B] + [AB]$. For each solution in the series, $[A_{tot}]$ and $[B_{tot}]$ were known, and the complex concentration was expressed as

$$[AB] = \frac{[A][B]}{K_d}. \quad (5)$$

Given these relations, the concentrations of the monomers may be expressed as

$$[A] = \frac{[A_{tot}]}{\left(1 + \frac{[B]}{K_d}\right)}; \quad (6)$$

$$[B] = -\frac{1}{2}\Big\{([A_{tot}] - [B_{tot}] + K_d) - \big\{([A_{tot}] - [B_{tot}] + K_d)^2 + 4[B_{tot}]K_d\big\}^{\frac{1}{2}}\Big\}. \quad (7)$$

Further discussion of the equilibrium relations used in this work may be found in the Supporting Material.

For the Method of Continuous Variation, stock solution concentration can impact data quality (12). However, as the absolute concentration of the proteins is taken into account, the K_d will not be under- or overestimated by nonoptimal stock concentrations. An appropriate stock solution concentration realizes an increase in r_h that is large enough to accurately detect. This typically means the stock concentration must be on the order of K_d, preferably $>K_d$. If the stock concentration is too low, there will be no detectable increase in r_h. Very high K_d values, i.e., weak interactions, may require high concentrations to detect the interaction. The limits of detection of this method vary with protein size and the stoichiometry of the interaction. Detection limits of the Wyatt DLS plate reader used for this research were 0.125 g L^{-1} for a 14.4-kDa protein, i.e., 1.8 kDa g L^{-1}. For a 150-kDa protein, this corresponds to a 10 μg mL^{-1} stock concentration. For unknown protein systems, the lowest concentration limit of the DLS instrument should initially be used for the stock concentration. Combining the results of several concentrations is of course beneficial, although not required.

For experiments involving interaction of nonidentical proteins, radii of monomers were measured via DLS under conditions for which they were known to not self-associate, based on earlier static light scattering experiments (data not shown). All monomer radii were fixed to those previously determined values during fitting. Fixing the monomer radii, rather than leaving them as free parameters in the fit, naturally resulted in lower uncertainty in the fit parameters of interest. Without such a priori knowledge, any self-association of the monomers can be tested separately, as shown in Fig. 1. If self-association is observed, it may be included in the modeling.

Measurement of complex radii was not so straightforward. For complexes that rapidly equilibrate with the monomer species, the complex always exists in solution in some equilibrium with monomer species, making isolation challenging if not impossible, and preventing direct measurement of the complex radii. However, complex radii may be calculated or modeled in various ways, or left as free parameters when fitting. There are literature data (11,18–20) that indicate a relation between r_h and molar mass, M, for globular protein monomers, which may be parameterized as $r_h = a_0 M^{1/\alpha}$ (Fig. S3). For solid spheres, α is 3. For globular protein monomers, the literature reports α values that vary between 2 and 3. As the molar mass of the complex is known, it is tempting to simply fix the r_h value of the complex based on such a relation to further reduce the number of free parameters. However, because there is significant variation of the α parameter in the literature data sets, and outliers are common, we chose to leave the radii of complexes as a free parameter when fitting. This is particularly appropriate given that there is no literature precedence that permits the conclusion that protein complexes have an r_h/M relationship identical to that of monomers. Accordingly, we expressed the radii of the complexes using a single parameter, α, as

$$r_{complex} = \left(\sum_i r_i^{\alpha}\right)^{\frac{1}{\alpha}}, \quad (8)$$

where r_i represents the radii of the constituent monomers. For systems containing only monomers and a single complex, this is equivalent to simply having the radius of the complex as a fit parameter. For systems with multiple complexes present simultaneously in solution, this relation constrains all complexes to have a similar change in density as a function of radius.

Although the α parameter may be determined by fitting DLS data alone, α is most accurately ascertained by simultaneous collection and fitting of both dynamic and static light scattering data from a concentration-gradient experiment. For protein solutions, static light scattering data analysis involves protein molar mass, not radii. Unlike monomer hydrodynamic radii, monomer molar masses are directly additive, and no α parameter is needed to calculate the molar mass of the complex. However, static data cannot currently be collected from microtiter plates. Consequently, the dual experiment must be performed using a flow-through light scattering instrument equipped with both static and dynamic light scattering detectors, as detailed in the Experimental procedures section. The simultaneous acquisition in the flow-through system required a sample quantity 1000 times that used for our lowest-volume stand-alone DLS measurements. However, requiring that both static and dynamic data analyses yield the same K_d resulted in a more highly constrained fit of the α parameter, thus reducing the uncertainty in determination of that variable. If the expenditure of sample is justified by the more precise determination of the parameters, the dual DLS and static light scattering experiment need be performed only once for the sample system. The resultant α parameter value can then be fixed in subsequent concentration-gradient DLS experiments.

Only one of the four systems characterized utilized the simultaneous collection and analysis of both static and dynamic light scattering for a more constrained α. For all other systems, α was left free in the fit of the DLS data. Most systems will be well fit without a simultaneous DLS/static light scattering experiment. In addition, the α parameter may be constrained, independent of any static light scattering experiment, to fall within a physically reasonable range, such as 2–3.

The r_{avg} values for every member of the concentration gradient, i.e., every member of the mole fraction series, were calculated using Eq. 8 in Eq. 4, and equilibria relations such as Eqs. 5–7. The calculated values were then fit against experimental data. The fit was weighted based on the r_{avg} standard deviation, which was calculated from the multiple measurements of each member of the concentration series. Best-fit parameters were determined by χ^2 minimization. Error bars for parameters determined by the fit were taken as the change in value required to increase the reduced χ^2 by 1 with all other parameters left free, yielding asymmetric upper and lower error bars (21).

RESULTS AND DISCUSSION

To demonstrate the efficacy of dynamic light scattering as a tool for the study of protein interactions, we chose to analyze several well-known systems. The association type differed for each system. First, the self-association of α-chymotrypsin at acidic pH was characterized. For this study, the association was studied at multiple salinities. The second system, α-chymotrypsin and bovine trypsin inhibitor, interacted in a 1:1 stoichiometry. Third, α-chymotrypsin and lysozyme were used as a negative control and, as expected, no interaction was detected. The last and most complex system was α-chymotrypsin, a serine protease, which interacted in a 2:1 stoichiometry with soybean trypsin inhibitor. Temperature studies were used to extract the ΔH° and ΔS° of the interaction. A small molecule that inhibited protein-protein binding was also identified, thus demonstrating the method's potential for studies involving small molecules. All experiments on this system were performed with high (10 μL) and low (1 μL) solution volumes.

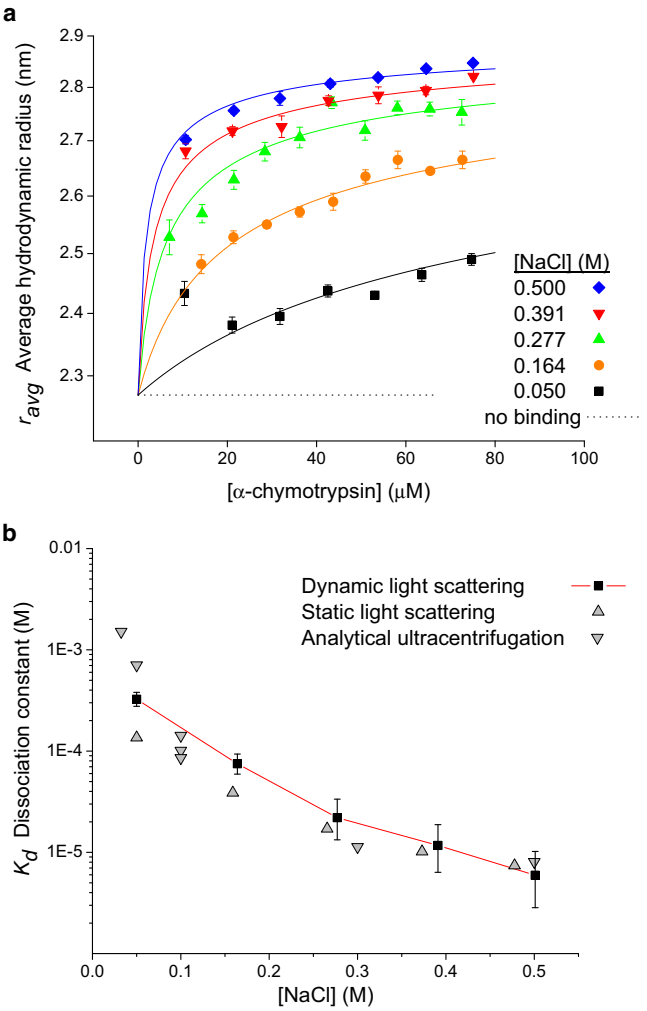

FIGURE 2 Characterization of α-chymotrypsin dimerization as a function of acidic buffer salinity. (*a*) Average hydrodynamic radius as a function of α-chymotrypsin concentration. Symbols represent measured data, fits are shown as solid lines, and error bars indicate the standard deviation (SD). The profile expected for no association is shown by the dotted line. (*b*) Equilibrium dissociation constants as a function of salinity. K_d values obtained from the DLS fits in *a* are shown in black, and values determined from alternate techniques in gray. Error bars represent the change in K_d value required to increase reduced χ^2 by 1.

At acidic pH, α-chymotrypsin was found to dimerize (Fig. 2 *a*). The self-association was measured at five separate sodium chloride concentrations, from 50 to 500 mM. All five data sets were fit simultaneously, with the monomer r_h set to the measured value of 2.27 nm. The fit yielded an α parameter of 2.78 (+0.13, −0.12), corresponding to a dimer hydrodynamic radius of 2.91 nm. In agreement with previous studies utilizing alternate techniques (5,22) (Fig. 2 *b*), K_d values were found to vary inversely with buffer salinity, as chymotrypsin is more prone to dimerize at higher salinities. When fitting this system, we were able to fix the monomer r_h to the value measured under nonassociating conditions, i.e., to the r_h value at nonacidic pH. Doing so reduced the number of free parameters, and thus reduced the uncertainty of the results. However, this a priori knowledge was not required. Essentially identical results were achieved when the monomer r_h was left as a free parameter. However, the error bars for the determined values increased. Table S1 shows a comparison of the results for the self-association of chymotrypsin with and without the monomer r_h fixed on the basis of a priori knowledge.

Since concentration-gradient DLS is based on an increase in hydrodynamic radii, the relative size of the interacting proteins is important; the technique is most sensitive with proteins of equivalent size. Accurate characterization currently requires that proteins *A* and *B* have r_h values within a factor of 2 of each other, i.e., molar masses within a factor of 5. Characterization of the α-chymotrypsin (25.5 kDa r_h = 2.27 nm)/bovine pancreatic trypsin inhibitor (6.5 kDa, r_h = 1.38 nm) interaction approached this limit of relative sizes. The maximum increase in the measured r_{avg} value at a mole fraction of 0.5 indicated an *n*:*n* complex (Fig. 3). Fitting gave 1:1 stoichiometry, with an α parameter of 2.85, corresponding to a dimer radius of 2.45 nm. Association increased with temperature. The K_d value at 25°C, 0.28 (+1.19, −0.25) μM, agreed with the literature value of 0.1 μM (4). As a negative control, chymotrypsin and lysozyme were also tested and showed no interaction (Fig. 3, *inset*).

α-Chymotrypsin and soybean trypsin inhibitor, with molar masses of 25.5 kDa and 21.5 kDa, respectively, both had measured r_h values of 2.27 nm. The proteins interacted

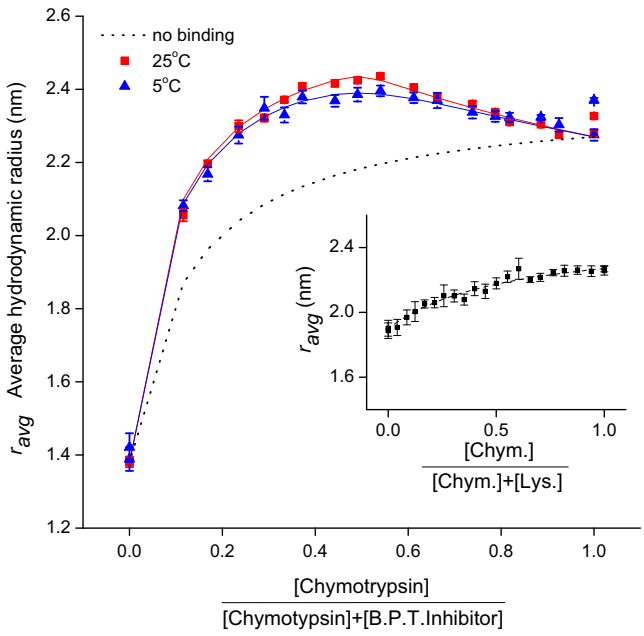

FIGURE 3 Characterization of a 1:1 α-chymotrypsin/bovine pancreatic trypsin inhibitor interaction at neutral pH at two temperatures. The profile expected for no association is shown by the dotted line. Fits are shown as solid lines. (*Inset*) Negative control of α-chymotrypsin and lysozyme, for which no association was expected or detected. Error bars show SD.

with a maximum increase at ~0.75 mol fraction (Fig. 4 *a*). The skew to higher chymotrypsin content indicated that multiple chymotrypsins were incorporated in the complex. Past inhibition studies/sedimentation equilibrium research involving chymotrypsin-soybean trypsin inhibitor have suggested that the soybean trypsin inhibitor is ''double-headed'', possessing two binding sites with comparable affinity for the enzyme (23). Concentration-gradient static light scattering studies (2) also reported two binding sites, with the addendum of an ''incompetent fraction'', a portion of the chymotrypsin incapable of binding the inhibitor. This incompetent fraction is not without precedence, as chymotrypsin is known to exist in at least two conformations, with only one conformation able to bind certain inhibitors (24,25).

The potential existence of an incompetent fraction complicated analysis. The maximum increase at 0.75 mol fraction could have resulted from a large incompetent fraction and a 1:1 association. However, the increase in r_{avg} to 3.3 nm (Fig. 4 *a*) was too great for this scenario, and 1:1 stoichiometry thus failed to fit the data. The data were fit with 2:1 stoichiometry with an incompetent fraction (reduced $\chi^2 = 1.1$), and also with 3:1 stoichiometry without an incompetent fraction (reduced $\chi^2 = 4.7$). Fit results and previous studies supported a 2:1 stoichiometry. We simultaneously acquired, and subsequently simultaneously fit, DLS and static light scattering data to constrain α as much as possible (Fig. 4 *c*). The determined α and incompetent fraction values were 1.98 (+0.16, −0.18) and 0.38 ± 0.03, respectively. This corresponded to a dimer radius of 3.22 nm, and a trimer radius of 3.95 nm. The values for α parameter and incompetent fraction were subsequently fixed to these values for all following stand-alone DLS measurements.

At 25°C, the average K_d was 0.53 (+0.11, −0.13) μM, in agreement with the literature value of 0.32 ± 0.16 μM (2). The sample plate was measured with the temperature sequence 25, 20, 15, 10, 5, 25, 30, 35, and 25 (°C). Association increased with temperature (Fig. 4 *b*). The multiple runs at 25°C (Fig. 4 *a*) confirmed that cycling the temperature did not impact binding ability. Also, absence of a gradual reduction of r_{avg} with time indicated that proteolytic activity of chymotrypsin did not appreciably affect either protein.

Thermodynamic information was obtained using a van't Hoff plot (Fig. 4 *d*). To validate low volume capability, two sets of experiments were performed with different sample volumes, 1 μL and 10 μL. ΔH° values were 12 ± 4 and 12 (+4, −5) kcal mol^{-1}, ΔS° values were 70 ± 14 and 70 (+16, −14) cal mol^{-1} K^{-1}, and reduced χ^2 values were 2.4 and 0.35, respectively. Agreement of the 1 μL and 10 μL results indicated that reduction in sample volume had minimal impact on data quality.

For the small-molecule study, chymotrypsin was pretreated with the irreversible small-molecule serine protease inhibitor, AEBSF. AEBSF reacts with the hydroxyl of the active-site serine residue to form a stable sulfonyl enzyme

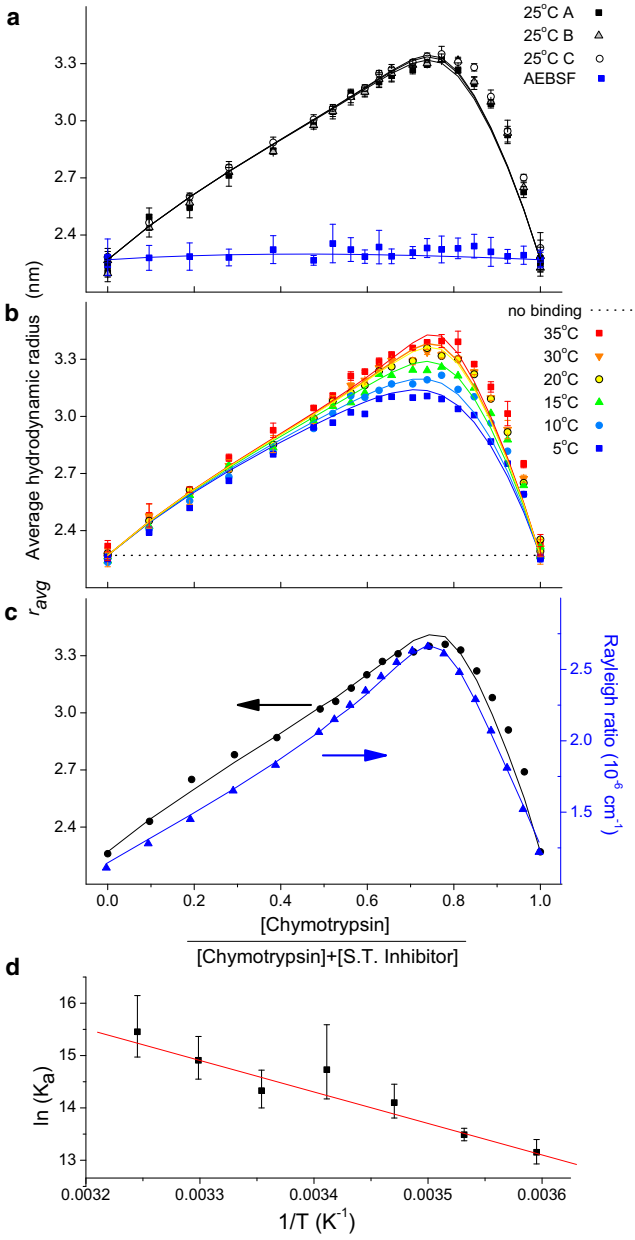

FIGURE 4 Characterization of a 2:1 α-chymotrypsin/soybean trypsin inhibitor interaction at neutral pH as a function of temperature. Data are presented as r_{avg} versus mole fraction of 0–1, with the mole fraction being the total molar concentration of chymotrypsin divided by the molar concentrations of both chymotrypsin and soybean trypsin inhibitor, yielding a range from entirely soybean trypsin inhibitor (0) to entirely chymotrypsin (1). Symbols represent measured data; fits are shown as solid lines. (*a*) Control measurements and small-molecule inhibition study (AEBSF). (*b*) Association as a function of temperature. The profile expected for no association is shown by the dotted line. In *a* and *b*, the error bars indicate the SD. (*c*) Determination of α parameter and incompetent fraction by simultaneous collection of both static and dynamic light scattering data. Static light scattering data is shown in blue and DLS data in black. Symbols represent average values of data taken over a time interval of at least 30 s during injection of each gradient step. (*d*) van 't Hoff plot. K_a values from fits in *b* are shown in black. Error bars represent the change in K_a value required to increase reduced χ^2 by 1. Minimization of χ^2 was used to fit the data, yielding a slope of $-\Delta H^\circ/R$ and an intercept of $\Delta S^\circ/R$.

derivative (26). Unbound AEBSF was then removed from the chymotrypsin solution with a desalting column before testing. We speculated that as soybean trypsin inhibitor prevented proteolytic activity of chymotrypsin, the enzyme's active site may be involved in the protein-protein binding site.

In contrast to untreated chymotrypsin, the AEBSF-treated chymotrypsin did not associate with the soybean trypsin inhibitor (Fig. 4 *a*). As the molar mass of AEBSF (240 g mol^{-1}, $r_h \sim 0.2$ nm) differed by more than a factor of 5 from that of chymotrypsin, (25,500 g mol^{-1}, $r_h = 2.27$ nm), their binding did not result in a measurable change in r_h. The chymotrypsin-AEBSF complex retained the r_h of the uninhibited protein, 2.27 nm (Fig. 2 *a*). As only chymotrypsin-AEBSF and soybean trypsin inhibitor (2.27 nm) were present in solution, the measured r_h was 2.27 over the entire mole fraction range.

This complete elimination of the protein-protein association suggests that the chymotrypsin active-site serine is involved in the binding of the soybean trypsin inhibitor protein. Alternatively, the binding of AEBSF may have induced a conformational change in the enzyme that prohibited the protein-protein association. This was a clear demonstration of how the impact of small molecules on protein associations may be studied without the complication of an altered protein radius. AEBSF was known to inhibit proteolytic activity of chymotrypsin, but the inhibition of the enzyme's interaction with other proteins was heretofore unknown.

SUMMARY

Concentration-gradient DLS was used to characterize four protein systems. Of the four, three demonstrated specific interaction, each with a distinct stoichiometry: 0:2, 1:1, or 1:2. The negative control evidenced no interaction. Table 1 summarizes all measured K_d values, which spanned more than three orders of magnitude. We were able to measure the response to environmental conditions such as buffer salinity and temperature, as well as the thermodynamics of the association. Measured values were shown to be constant down to the smallest solution volume of 1 μL. Although not optimized for reduced sample use, these nondestructive experiments used only 426 pmol of protein (20 1-μL solutions at 500 μg/mL, minimum molar mass of 6.5 kDa). As the intensity of scattered light is proportional to the product of molar mass squared and molar concentration, similar studies with antibodies (150 kDa) should require only 2.9 fmol (20 1-μL solutions at 22 μg/mL).

For one of the systems studied, concentration-gradient DLS was combined with concentration-gradient static light scattering to determine the α parameter. This measurement used 1000× the quantity of sample over stand-alone DLS measurements. However, after the one-time expenditure of sample, subsequent low-volume stand-alone DLS results had reduced uncertainty.

A significant limitation of concentration-gradient DLS, namely, that the molar mass of the interacting protein must

TABLE 1 Summary of results

α-Chymotrypsin/soybean trypsin inhibitor, 10 μL sample volume			α-Chymotrypsin/soybean trypsin inhibitor, 1 μL sample volume		
T (°C)	K_d (μM)	+, − error (μM)	T (°C)	K_d (μM)	+, − error (μM)
5	1.94	0.49, 0.42	5	2.07	0.50, 0.43
10	1.39	0.17, 0.16	10	1.89	0.20, 0.19
15	0.75	0.26, 0.22	15	0.50	0.20, 0.17
20	0.40	0.30, 0.23	20	0.66	0.35, 0.28
25	0.60	0.23, 0.19	25	0.99	0.30, 0.25
25	0.48	0.18, 0.15	25	0.67	0.21, 0.18
25	0.52	0.25, 0.20	25	0.64	0.26, 0.22
30	0.34	0.14, 0.12	30	0.40	0.15, 0.13
35	0.19	0.12, 0.10	35	0.09	0.10, 0.07
AEBSF, 25	NB	NB			
α-Chymotrypsin/bovine pancreatic trypsin inhibitor			α-Chymotrypsin self-association		
T (°C)	K_d (μM)	+, − error (μM)	[NaCl] (mM)	K_d (μM)	+, − error (μM)
5	15.68	12.56, 8.74	50	325.24	55.48, 48.18
6	5.40	7.19, 4.41	164	74.95	18.44, 15.75
15	2.25	1.39, 1.08	277	21.99	11.5, 8.71
25	0.28	1.19, 0.25	391	11.72	7.07, 5.35
			501	5.94	4.26, 3.1
α-Chymotrypsin/lysozyme					
T (°C)	K_d (μM)	+, − error (μM)			
25	NB	NB			

NB, no binding detected.

be no more than five times larger or smaller than its binding partner, has a silver lining. As the protein hydrodynamic radius is not altered by the binding of a small molecule, the impact of small molecules on protein-protein interactions may generally be studied without complication of an altered protein radius.

Although all experiments presented here involved protein-protein interactions, the method is applicable to a much broader class of reactants. Given the lack of a protein-specific labeling or immobilization procedure, extension of the technique to other biomolecules, such as tRNA, is straightforward. Also, in conjunction with other techniques, e.g., small-molecule screening or site-directed mutagenesis, concentration-gradient DLS may enable the identification of residues involved in protein molecular recognition. In this manner, concentration-gradient DLS may be used not only to characterize biomolecular interactions, but also to explain them.

SUPPORTING MATERIAL

Further discussion of modeling and theory used in this article, three figures, a table, and references are available at http://www.biophysj.org/biophysj/supplemental/S0006-3495(09)01609-9.

The photographic image shown in Fig. 1 is courtesy of Stuart Ponder of somethingclickedphotography.com.

REFERENCES

1. Yamaguchi, T., and K. Adachi. 2002. Hemoglobin equilibrium analysis by the multiangle laser light-scattering method. *Biochem. Biophys. Res. Commun.* 290:1382–1387.
2. Attri, A. K., and A. P. Minton. 2005. Composition gradient static light scattering: a new technique for rapid detection and quantitative characterization of reversible macromolecular hetero-associations in solution. *Anal. Biochem.* 346:132–138.
3. Attri, A. K., and A. P. Minton. 2005. New methods for measuring macromolecular interactions in solution via static light scattering: basic methodology and application to nonassociating and self-associating proteins. *Anal. Biochem.* 337:103–110.
4. Kameyama, K., and A. P. Minton. 2006. Rapid quantitative characterization of protein interactions by composition gradient static light scattering. *Biophys. J.* 90:2164–2169.
5. Larkin, M. I., and P. Wyatt. 2010. Light scattering techniques and their application to formulation and aggregation concerns. *In* Formulation and Process Development Strategies for Manufacturing of a Biopharmaceutical. F. Jameel and S. Hershenson, editors. Wiley and Sons, New York, In press.
6. Pecora, R., editor. 1985. Dynamic Light Scattering: Applications of Photon Correlation Spectroscopy. Plenum Press, New York.
7. Herbert, T. J., and F. D. Carlson. 1971. Spectroscopic study of the self-association of myosin. *Biopolymers.* 10:2231–2252.
8. Wang, C. C., N. C. Ford, Jr., and M. J. Fournier. 1981. Laser light-scattering analysis of the dimerization of transfer ribonucleic acids with complementary anticodons. *Biopolymers.* 20:155–168.
9. Lunelli, L., E. Bucci, and G. Baldini. 1993. Electrostatic interactions in hemoglobin from light scattering experiments. *Phys. Rev. Lett.* 70: 513–516.
10. Berreta, S., G. Chirico, …, G. Baldini. 1997. Photon correlation spectroscopy of interacting and dissociating hemoglobin. *J. Chem. Phys.* 106:8427–8435.
11. Sharma, P., D. Rajalingam, T. K. S. Kumar, and S. Singh. 2008. A light scattering study of the interaction of fibroblast growth factor (FGF) with its receptor. *Biophys. J.* L71–L73.
12. Huang, C. Y. 1982. Determination of binding stoichiometry by the continuous variation method: the Job plot. *Methods Enzymol.* 87: 509–525.
13. Job, P. 1928. Formation and stability of inorganic complexes in solution. *Ann. Chim.* 9:113–203.
14. Koppel, D. E. 1972. Analysis of macromolecular polydispersity in intensity correlation spectroscopy: the method of cumulants. *J. Chem. Phys.* 57:4814–4820.
15. Provencher, S. W. 1979. Inverse problems in polymer characterization: direct analysis of polydispersity with photon correlation spectroscopy. *Makromol. Chem.* 180:201–209.
16. Brown, J. C., P. N. Pusey, and R. Dietz. 1975. Photon correlation study of polydisperse samples of polystyrene in cyclohexane. *J. Chem. Phys.* 62:1136–1144.
17. Wyatt, P. J. 1993. Light scattering and the absolute characterization of macromolecules. *Anal. Chim. Acta.* 272:1–40.
18. Claes, P., M. Dunford, …, P. Vardy. 1992. An on-line dynamic light scattering instrument for macromolecular characterization. *In* Laser Light Scattering in Biochemistry. S. E. Harding, D. B. Sattelle, and V. A. Bloomfield, editors. The Royal Society of Chemistry, Cambridge. 69.
19. van Holde, K. E., W. C. Johnson, and P. S. Ho. 1998. Principles of Physical Biochemistry. Prentice Hall, Upper Saddle River, NJ. 200–203.
20. Tanford, C. 1961. Physical Chemistry of Macromolecules. Wiley, New York. 356–381.
21. Flannery, B. P., S. A. Teukolsky, and W. T. Vetterling. 1988. Numerical Recipes in C. Press Syndicate of the University of Cambridge, Cambridge, United Kingdom. 517–556.
22. Aune, K. C., L. C. Goldsmith, and S. N. Timasheff. 1971. Dimerization of α-chymotrypsin. II. Ionic strength and temperature dependence. *Biochemistry.* 10:1617–1622.
23. Bösterling, B., and U. Quast. 1981. Soybean trypsin inhibitor (Kunitz) is doubleheaded. Kinetics of the interaction of α-chymotrypsin with each side. *Biochim. Biophys. Acta.* 657:58–72.
24. Fersht, A. R. 1972. Conformational equilibria in α-and δ-chymotrypsin. The energetics and importance of the salt bridge. *J. Mol. Biol.* 64: 497–509.
25. Erlanger, B. F., and R. A. Sack. 1970. Operational normality of α-chymotrypsin solutions by a sensitive potentiometric technique using a fluoride electrode. *Anal. Biochem.* 33:318–322.
26. Powers, J. C., J. L. Asgian, …, K. E. James. 2002. Irreversible inhibitors of serine, cysteine, and threonine proteases. *Chem. Rev.* 102: 4639–4750.